

Science and Technology for the Built Environment



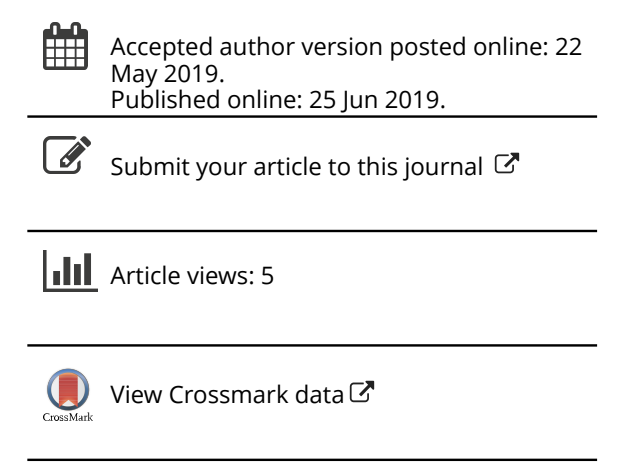
ISSN: 2374-4731 (Print) 2374-474X (Online) Journal homepage: https://www.tandfonline.com/loi/uhvc21

Numerical optimization of integrated passive heating and cooling systems yields simple protocols for building energy decarbonization

Alexandra R. Rempel & Serena Lim

To cite this article: Alexandra R. Rempel & Serena Lim (2019): Numerical optimization of integrated passive heating and cooling systems yields simple protocols for building energy decarbonization, Science and Technology for the Built Environment, DOI: 10.1080/23744731.2019.1620578

To link to this article: https://doi.org/10.1080/23744731.2019.1620578



Science and Technology for the Built Environment, (2019) $\mathbf{0}$, 1–11

Copyright © 2019 ASHRAE.

ISSN: 2374-4731 print / 2374-474X online DOI: 10.1080/23744731.2019.1620578





Numerical optimization of integrated passive heating and cooling systems yields simple protocols for building energy decarbonization

ALEXANDRA R. REMPEL^{1*} D AND SERENA LIM²

Passive heating and cooling systems have the potential to reduce space-heating and space-cooling loads in buildings significantly, with minimal embodied energy investment and extremely low operational energy demand. Excellent performance requires movable insulation, operable shading, operable vents, and other adjustable elements, but effective methods for controlling their operation have not yet been established. In particular, the numerical optimization of interdependent passive heating and cooling parameters to maintain thermal comfort has not yet been demonstrated; development of simplified control strategies has not been explored; and resulting load reductions have not been estimated. Here, we investigate these problems in planning for the adaptive reuse of an historic brick office building in the Mediterranean climate of Berkeley, California. Using Hooke-Jeeves and particle-swarm optimizations of passive system parameters in a field-validated EnergyPlus model, constrained to develop monthly schedules responding only to time or temperature, we find that near-optimal configuration and control of passive solar collection eliminate over half of the baseline heating load; likewise, well-controlled shading and natural ventilation eliminate ~80% of the cooling load. Together, these results reveal the magnitude of the passive space-conditioning resource in this energy-intensive region and demonstrate the power of simple, effective operational strategies to realize substantial energy savings.

Introduction

Two recent landmark reports describe the unprecedented changes for the future unless greenhouse gas emissions are immediately and sharply curtailed: a new special report from the Intergovernmental Panel on Climate Change notes the global expansion of severe weather, fires, and flooding (Hoegh-Guldberg et al. 2018), while the U.S. Fourth National Climate Assessment (U.S. Global Change Research Program 2018) predicts a dramatic contraction in the U.S. economy in the coming decades without swift action. Because the United States is a leading global contributor to climate change, and because local and regional actions can progress more rapidly than federal policy, specific and practical methods for

Received December 28, 2018; accepted May 3, 2019 Alexandra R. Rempel, PhD, MArch, is an Assistant Professor. Serena Lim, MArch, is a Graduate Research Fellow.

*Corresponding author e-mail: arempel@uoregon.edu Color versions of one or more of the figures in the article can be found online at www.tandfonline.com/uhvc.

ⓑ Supplemental data for this article can be accessed on the publisher's website at https://doi.org/10.1080/23744731.2019. 1620578

reducing emissions that are immediately adoptable by U.S. states and regions are urgently needed.

Currently, fossil-fueled space heating and cooling consume over half of all energy used in U.S. buildings, emitting an estimated 500 million metric tons of CO₂ each year (U.S. Energy Information Administration 2018a). California, with about 12% of the U.S. population, is the second-greatest greenhouse gas emitting state (U.S. Energy Information Administration 2018b), although per-capita consumption is among the lowest due to long-term renewable energy and energy efficiency efforts (California Energy Commission 2018). To phase out remaining emissions, California's governor recently signed an executive order establishing a statewide goal of carbon neutrality by 2045 (Executive Order B-55-18 2018). This was soon discovered to require the decarbonization of space heating in the state, approximately 90% of which is provided by natural gas combustion (Hopkins et al. 2018; U.S. Energy Information Administration 2018b); likewise, space cooling needs are projected to grow, particularly in coastal areas, increasing competition for renewable electricity supplies (Ackerly et al. 2018).

Among these coastal areas, the San Francisco Bay metropolis is home to nearly 9 million people (World Population Review 2018) and part of an emerging Northern California

¹Environmental Studies Program, University of Oregon, Eugene, OR 97403, USA

²Department of Architecture, University of Oregon, Eugene, OR, USA

megaregion expected to surpass 20 million by 2050 (Regional Plan Association 2018). The region's Mediterranean climate (Köppen *Csb*; Peel et al. 2007) has wet, cloudy winters perceived as having limited potential for passive solar heating (e.g., DeKay and Brown 2013; Duffie and Beckman 2013) and warm, dry summers expected soon to require air conditioning (Ackerly et al. 2018). We focus our efforts here to reveal the potential for passive heating and cooling resources to meet space-conditioning needs in a region in which they are typically dismissed, promoting independence from fossil fuels while maintaining thermal comfort throughout the year.

Operable elements improve passive system performance significantly, and their control is of widespread interest: recent efforts have investigated contrasting control schemes for natural ventilation (Schulze and Eicker 2013; Wang et al. 2009), night ventilation of thermal mass (Chahwane et al. 2011; Santamouris et al. 2010; Shaviv et al. 2001), shading (Littlefair et al. 2010; Tzempelikos and Athienitis 2007; Grynning et al. 2014; Karlsen et al. 2016), and natural ventilation and shading together (van Moeseke et al. 2007; Ochoa and Capeluto 2008), finding in each case that the choice of strategy greatly affects system effectiveness. However, these cases each pre-selected both control parameters (e.g., indoor air temperature; global horizontal radiation) and threshold values (e.g., 25 °C; 50 W/m²). While the chosen values had logical bases, they were not shown to be the best of all possible values, and evidence exists to suggest that optimal control strategies may, in some cases, be counter-intuitive (Rempel and Remington 2015). In addition, further exploration of such predetermined schemes has given rise to involved networks of control rules that require computational systems to sense and respond to weather and building conditions (e.g., Schulze et al. 2018; Karlsen et al. 2016), appropriate for some large buildings but impractical for small buildings and dwelling units.

Numerical optimizations able to explore complete solution spaces have the potential to reveal optimal control strategies within acceptable limits of complexity, but they have not yet been applied to the development of straightforward integrated passive system control strategies. Genetic algorithms, neural networks, and numerous parametric studies have, however, been used to inform choices of fixed elements of passive systems, including glazing orientation and type, wall composition, overhang depth, etc., reviewed by Stevanović (2013). While some of these efforts considered the presence vs. absence of operable elements as optimizable elements, control parameters and thresholds were again preestablished. To our knowledge, only Rempel and Remington (2015) has previously optimized the selection of control parameters themselves (e.g., indoor air temperature; global horizontal radiation) and the values of the control thresholds (e.g., 25 °C; 50 W/m²) for signaling the operation of passive system components. However, that work addressed passive cooling alone, without imposing a lower temperature bound, and it did not estimate a cooling load reduction.

The current effort expands upon previous work by seeking optimal configurations and control schedules for passive heating and cooling systems operating together, maintaining adaptive thermal comfort and constrained to provide manageable monthly schedules, in a method suitable for buildings in all

climates. Application of this method to a field-validated model of an historic brick office building in Berkeley, California then reveals the annual heating and cooling load reductions possible in this and, by extension, numerous other existing buildings in this densely-populated area.

Materials and methods

Study site

Berkeley, California, on the eastern shore of San Francisco Bay, has a Mediterranean climate (Köppen *Csb*) with typical average monthly temperatures between 10 °C and 17 °C throughout the year and annual precipitation of approximately 700 mm concentrated in winter months (Western Regional Climate Center 2016; National Solar Radiation Data Base 2005). The winter is mild, long, and cloudy, characteristic of west-coast, marine-influenced climates (Peel et al. 2007), with eight months (October–May) exceeding the threshold of 60 heating degree-days (HDD) at a base temperature of 18.3 °C, above which a U.S. residential building of typical construction is expected to need heat (U.S. Energy Information Administration 2015; Figure 1).

The space investigated (Figure 2, Table 1) is one of two upper units of a two-story brick-and-timber row building in Berkeley's dense south downtown area, built in 1904, elongated in the east-southeast to west-northwest direction with party walls on the northernmost and southernmost sides. Solar access is provided primarily by a large central multipanel skylight, with lesser contributions by two smaller skylights; natural ventilation is available through operable windows on the shorter easternmost and westernmost walls, as well as operable panels of the large central skylight. It currently supports office activities but will soon undergo an adaptive reuse conversion into a dwelling.

EnergyPlus model assembly

The existing building was modeled as eight thermal zones representing each of the four main units and each of the four

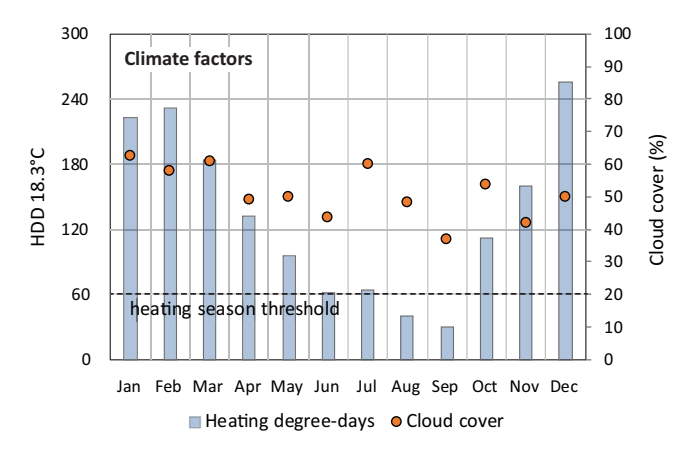


Fig. 1. Typical monthly heating degree-days at a base temperature of 18.3 °C in Berkeley, California, compared to the heating season threshold of 60 HDD_{18.3°C}/month and monthly average cloud cover.

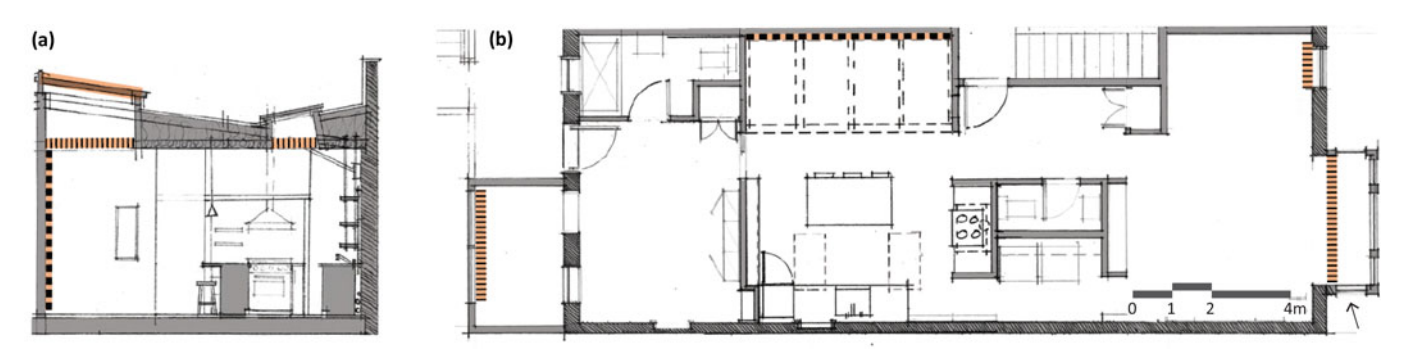


Fig. 2. Existing space in (a) section and (b) plan, with movable insulation locations indicated by fine dashes and interior brick thermal mass indicated by heavy dashes (Rempel and Lim 2018).

Table 1. Existing conditions and changes investigated.

Parameter	Existing condition	Changes
Floor area	98.25m ²	
Orientation	17° W of true south (i.e., 197°)	
Roof assembly	Bitumen membrane o/ 75 mm insulation board o/ 13 mm plywood sheathing o/ 154 mm batt insulation o/ 16 mm gypsum board	
Wall assemblies	N, S: adiabatic (party walls); E, W: 330 mm solid brick (exterior); Porch: wood siding o/13 mm plywood sheathing o/ 154 mm batt insulation o/13 mm plywood o/16 mm gypsum board	
Floor assembly	25 mm Douglas fir o/19 mm wood subfloor o/154 mm batt insulation o/19 mm gypsum board o/conditioned space	
Window assemblies	E, W: Double clear glazing, wood frame (7.8 m ² , 1.0 m ²); W porch: Double clear glazing, aluminum frame (3.9 m ²); Small skylights: Single clear glazing, aluminum frame (0.74 m ²)	
Skylight assembly	Acrylic dome, 7.2m^2 : $T_{\text{vis}} = 0.53$, SHGC = 0.5, U = 3.2 W/m ² K	Glazing (SHGC = 0.67; U = $3.5 \text{W/m}^2 \text{K}$; $T_{\text{vis}} = 0.72$), Tilt
Movable insulation	None	Material ($k = 0.03$ W/mK, 2.54 cm thick); schedule
Shading	None	Material ($T_{vis} = 0.3$, $T_{sol} = 0.3$); schedule
Infiltration	0.75 ACH	, 301
Thermal mass	Exterior brick walls only	Addition of interior brick wall (0.89 W/mK, 1920 kg/m ³ , 790 J/kgK)
Natural ventilation	Operable E, W windows (2m ²); operable skylights (2 m ²)	Temperature thresholds
Internal gains	Office: People: 3 adults; Electric power density (lighting, electronics, baseboard heat) = 50 W/m ² ; 8 a.m5 p.m. weekday occupancy	Household: People: 2 adults; Electric power density (lighting, electronics): 2 W/m ² ; 24-h occupancy

attached but thermally distinct balconies. All geometry was created in Euclid v0.9.3 (Big Ladder Software 2017) for simulation in EnergyPlus v8.7 (U.S. Department of Energy 2016b), and materials and constructions were entered directly into the IDF Editor using known or typical material values (ASHRAE 2013; Table 1). Window and skylight glazing assemblies and framing were modeled in WINDOW 7.6 (Lawrence Berkeley National Laboratory 2017); angle- and wavelength-dependent properties were then exported and referenced by EnergyPlus using Construction:WindowDataFile objects. Opening and crack areas were measured directly for infiltration estimation

by EnergyPlus, yielding an estimate of approximately 0.75 ACH; internal heat gain sources included occupants, electric lighting, computer equipment, and baseboard heating, each following an approximate 8 a.m.–5 p.m. weekday occupancy schedule.

Model evaluation

Within the main living space, air (dry-bulb) temperature, relative humidity, and illumination were monitored at 30-min intervals in triplicate for two weeks in December, 2017

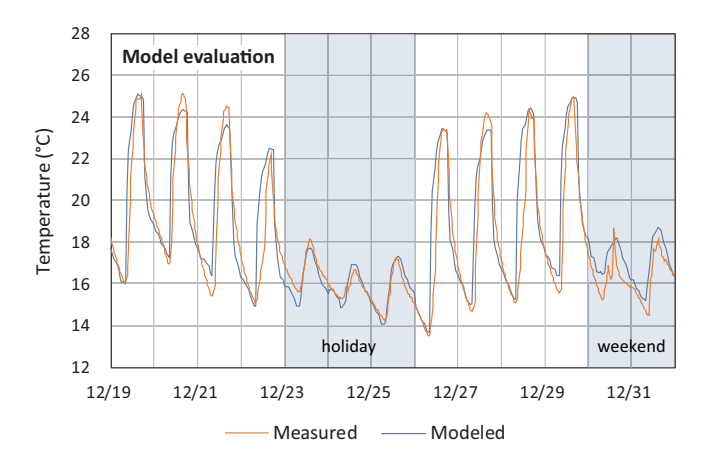


Fig. 3. Comparison of modeled with measured indoor air temperatures in December 2017; the model predicted about 80% of the variability in the measurements ($R^2 = 0.793$).

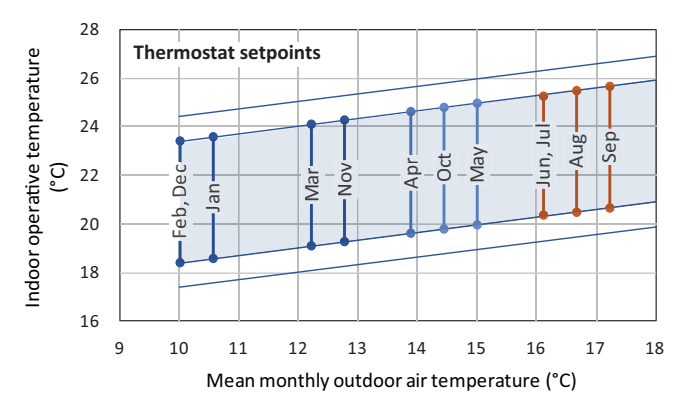


Fig. 4. Thermostat setpoints, by month, corresponding to the upper and lower bounds of acceptability to 90% of the population (shaded area) in the ASHRAE 55-2017 Adaptive Comfort Model (ASHRAE 2017). The outer boundaries show the upper and lower bounds of 80% acceptability.

with UA-002-08 pendant and U12-013 dataloggers; two outdoor positions, the stairwell, and the porch were monitored as well with UA-002-08 loggers (Onset Computer Corp.). Illumination was measured to reveal occupancy patterns, informing the model's occupancy schedule, and indoor relative humidity was measured to reveal whether activities such as cooking or humidifier use occurred during the measurement period. Dataloggers were factory-calibrated in 2016, showing temperature measurement uncertainties of ±0.53 °C from 0° to

 $50\,^{\circ}\text{C}$ (±0.95 $^{\circ}\text{F}$ from 32° to $122\,^{\circ}\text{F})$ and annual drift of less than $0.1\,^{\circ}\text{C}$ (0.2 $^{\circ}\text{F}).$

Archived 2017 weather data (air temperature, dew point temperature, relative humidity, atmospheric pressure, wind direction, wind speed, cloud cover) were obtained from the Oakland Metropolitan Airport weather station KOAK (WBAN 23230), and global horizontal, direct normal, and diffuse horizontal solar radiation data were obtained from SolarAnywhere (solaranywhere.com) through an academic license.

To evaluate the fidelity of the EnergyPlus model, weather data for December 2017 were substituted for typical December data in the Oakland, CA TMY3 weather file. Simulation using this "observed" weather file predicted approximately 80% of the variability in field measurements ($R^2=0.793$; Figure 3), providing confidence that all of the significant pathways for heat gain, loss, and storage in the study unit had been represented faithfully in the model.

Baseline model configuration

From the model of the existing building, a "baseline" model was created for evaluation of passive system performance in the intended dwelling configuration. Internal gains due to people, lights, and equipment were adjusted from office levels to the somewhat lower levels expected of a live-work household, and full-time occupancy was added (Table 1). Baseboard heating was removed, and an Ideal Loads Air System was added to quantify heating and cooling loads independent of mechanical system efficiency. This system, in turn, was controlled by a thermostat (Figure 4) set to maintain indoor operative temperatures within the 90% acceptability limits of the ASHRAE adaptive thermal comfort zone, which defines the relationship between average monthly outdoor air temperatures and comfortable indoor temperatures for naturally-conditioned spaces such as this one (ANSI/ASHRAE 2017).

Optimizations

The goal of each optimization was to reveal the value of a particular passive heating or cooling parameter (e.g., thermal mass thickness) that minimized the sum of annual heating and cooling loads, within the limits we imposed. First, movable insulation and shading elements were added to the baseline model using <code>WindowProperty:ShadingControl</code> objects as <code>InteriorShade</code> configurations and referenced by <code>FenestrationSurface:Detailed</code> objects; top, bottom, left-side, and right-side opening multipliers of 0.05 represented the

Table 2. Optimization parameters.

Parameter	Initial step size	Range	Optimum
Skylight tilt	5°	0°–90°	40°
Movable insulation hour of activation/ retraction	1 hour	12 a.m.–11 p.m.	Varies monthly
Shading hour of activation/retraction	1 hour	12 a.m.–11 p.m.	Varies monthly
Thermal mass wall thickness	5 cm	0 cm-30 cm	25cm
Natural ventilation outdoor temperature maximum	10 °C	20 °C–38 °C	Varies monthly
Natural ventilation indoor temperature minimum	10 °C	16 °C–30 °C	Varies monthly

capture of material edges within tracks or channels. Addition of the brick thermal mass wall was represented with a new interior wall construction, and natural ventilation was represented by *ZoneVentilation:WindAndStackOpenArea* objects and controlled by Minimum Indoor and Maximum Outdoor temperature scheduling.

Optimizations were then conducted by GenOpt v3.1.1, an open-source optimization engine for EnergyPlus (Bushnell 1990; Wetter 2016) that has shown success in recent work (Djuric et al. 2007; Kämpf et al. 2010; Rempel and Remington 2015; Rahadian and Alhamid 2015). In the optimizations shown in Table 2, GenOpt varied the value of each parameter of interest according to specified guidelines and a specified optimization algorithm, substituting successive values into the EnergyPlus template file and evaluating EnergyPlus simulation results until the value was found that minimized the annual sum of heating and cooling loads. The Hooke-Jeeves pattern search algorithm was used for continuous variables, and the Kennedy-Eberhart binary particle swarm optimization was used for discontinuous variables, according to Wetter and Wright (2003). After a step of the initial size was no longer productive, the step size was reduced by half, and then halved repeatedly until three successive steps showed no further improvement. To further reduce the likelihood that global minima were missed, each optimization was also conducted with multiple starting points and step sizes. Because software limitations prevented all optimizations from being conducted simultaneously, elements were optimized sequentially, beginning with those that functioned most independently. All simulations used the most recent version of typical meteorological year weather data (TMY3) for nearby Oakland, California (National Solar Radiation Data Base 2005).

Results and discussion

Baseline performance

To maintain conditions within the 90% acceptability limits of the adaptive thermal comfort zone (Figure 4), under typical (TMY3) Oakland CA weather conditions, the baseline building configuration (i.e., existing building modified for live-work occupancy) required 5.6 MWh (20.1 GJ) of sensible heating and cooling energy annually (Figure 5a). Latent loads were neglected because relative humidity does not affect adaptive thermal comfort boundaries (ANSI/ASHRAE 2017) and because Mediterranean climates have characteristically dry summers, diminishing the need to dehumidify during the cooling season.

Window solar gain, primarily through the large unshaded central skylight, constituted the largest heat gain pathway, converting the heating-season months of April and May into net cooling months and increasing summer cooling loads as well, while infiltration and window heat losses contributed most to heat loss pathways (Figure 5b). During the cool months of October–May, monthly heating loads (Figure 5a) were often higher than net monthly heat losses (Figure 5b) because, in the baseline configuration, daytime solar gains

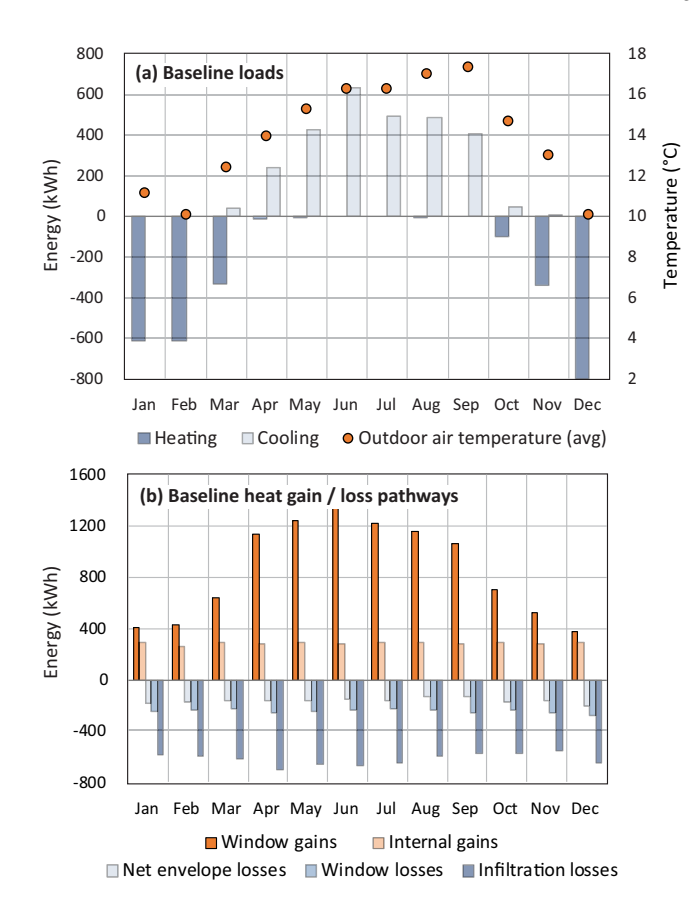


Fig. 5. Baseline building performance, including (a) monthly sensible heating and cooling energy required to maintain indoor operative temperatures within the adaptive comfort thermostat setpoints, compared to mean monthly outdoor air temperature, and (b) envelope heat gain and loss pathways, showing prominent heat gains through the existing skylight and prominent losses through windows and infiltration.

were not stored in such a way that they could offset nighttime losses effectively.

Skylight glazing tilt

Redesign efforts first explored passive heating decisions because these were expected to increase cooling loads, requiring accommodation by subsequent cooling decisions. In a building without south-facing walls or windows, passive solar heating might have been dismissed as a possibility, given the emphasis of long-standing passive solar design literature on the need for vertical glass to collect energy from "low" winter sun angles (e.g., Lechner 2014; DeKay and Brown 2013; Goswami et al. 2000; Balcomb et al. 1984).

To the contrary, however, recent work has shown that tilted glazing greatly improves solar collection in cloudy winter climates (Rempel et al. 2013): since clouds scatter both visible and infrared photons toward the top of the sky dome, solar energy emanates from altitudes higher than the sun's position under partly cloudy to overcast conditions (Eymet et al. 2004; International Commission on Illumination 2003; Perez et al. 1990). Because the typical Berkeley-area cloud cover is

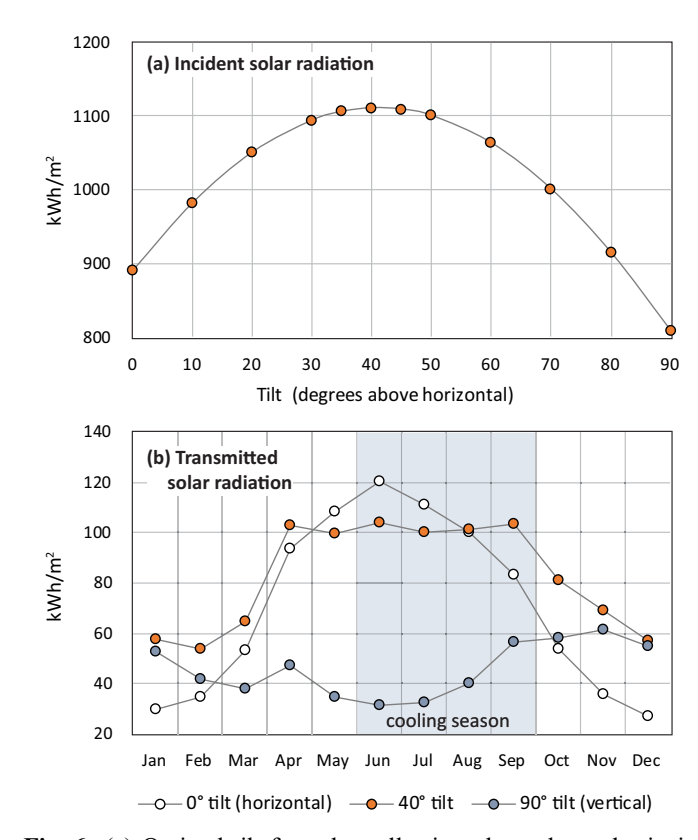


Fig. 6. (a) Optimal tilt for solar-collecting glass, shown by incident solar radiation during the heating season months on surfaces of specified tilt to be approximately 40° above horizontal, and (b) monthly transmitted solar radiation through double-clear glazing (Table 1) tilted at 40° compared to that through conventionally-recommended vertical (90°) glazing. Transmission through horizontal glazing is shown for comparison.

50% or greater in all heating-season months except November (Figure 1), diffuse radiation was expected to be an important component of the solar resource. Incident solar radiation on surfaces of varying tilt was therefore estimated, using the Perez model (Perez et al. 1990) with Oakland TMY3 weather data, revealing that a tilt of 40° would intercept the greatest quantity of energy during the heating season (Figure 6a).

Examination of the monthly components of this incident solar resource showed that the optimally-tilted glazing most improved upon vertical glazing during months with longer days (March, April, May, and October), effectively shortening the heating season (Figure 6b). Although incident solar radiation on the optimally-tilted surface was predicted to be ~35% greater than that on a vertical surface (Figure 6a), the solar radiation transmitted through the glass was expected to be almost 50% greater in total, and more than 100% greater in some months (Figure 6b), because the proportion of energy reflected away from a window increases as the angle of incidence becomes shallower (Carmody et al. 2007).

Replacement of the original skylight's diffusing acrylic dome (Table 1) with double-clear glazing of optimal tilt did not in itself appreciably diminish the heating load, since thermal mass and movable insulation were not yet present to retain

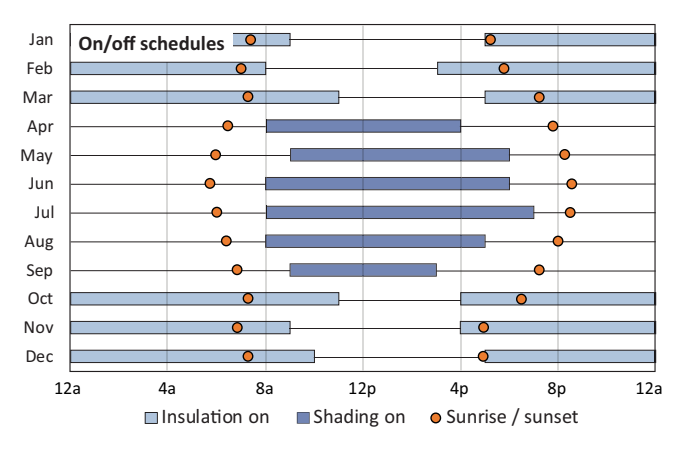


Fig. 7. Optimal hours for use of movable insulation and shading (bars), as well as hours of sunrise and sunset (circles), showing that movable insulation was optimally retracted several hours after sunrise and redeployed before sunset in most heating-season months, and that shading was optimally retracted before sunset in the cooling season, remaining retracted until several hours after sunrise.

the collected heat; moreover, this change increased the summer cooling load, as expected and as discussed below.

Movable insulation and shading schedules

The second redesign effort therefore investigated the benefits available from optimal scheduling of movable insulation and interior shading, applied to all windows. The thermal properties of these materials ($k\!=\!0.03$ W/mK for movable insulation; $T_{\rm vis}=0.3$ for interior roller blinds) reflected the choice of inexpensive, conveniently operable, commercially-available products.

Conventional wisdom assumes that movable insulation is needed only "at night," that is, the hours between sunset and sunrise (e.g., van Moeseke et al. 2007; Stevanović 2013; U.S. Department of Energy 2016a). Questioning this assumption, optimizations here sought hourly schedules, by month, for deployment and retraction that minimized the annual sum of heating and cooling loads. Results showed that movable insulation was, in fact, optimally deployed one or more hours before sunset in most heating-season months and that it optimally remained in place for several hours after sunrise (Figure 7).

This revealed an important distinction between illumination (i.e., day/night designation) and heat flux through window glass. Since the coldest hours of the day often occurred near sunrise, as they did in February, sunrise often preceded net heat gain through the skylight by one or two hours (Figure 8a); as a result, movable insulation was optimally kept in place for several hours after sunrise, reducing heat loss by about 1/3 (Figure 8b). At the same time, net heat gain through the glass often ended (and net heat loss began) several hours before sunset, causing the movable insulation to require activation before sunset, as well. The only exceptions occurred in December and January, as unexpected consequences of the relatively low upper thermal comfort bounds in those months (Figure 4) and resulting attempts of the optimization algorithms to minimize overheating

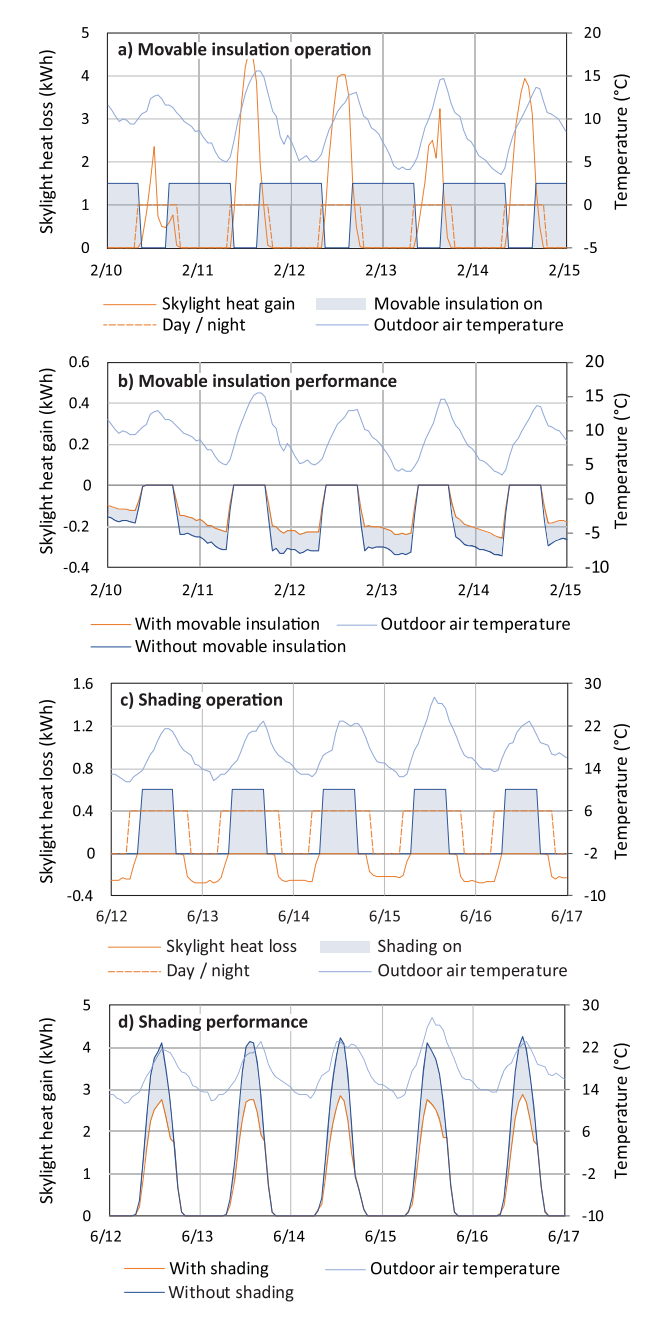


Fig. 8. Optimized movable insulation and shading performance for representative weeks in February and June, respectively, for the large central skylight. (a) Movable insulation (shaded areas) was optimally activated several hours before sunset, coinciding with a decline in skylight heat gain; similarly, it was optimally retracted only in the second hour after sunrise, when outdoor air temperatures had begun to rise. (b) Heat loss with and without movable insulation during a typical February week, illustrating the reduction in heat loss by $\sim 1/3$ achievable through the operation patterns shown above (Figure 7). (c) Shading (shaded areas) was optimally activated several hours after sunrise, when the skylight ceased to lose heat to the cool outdoor air; similarly, it was optimally retracted several hours before sunset, when skylight heat loss typically began again and continued throughout the night. (d) Heat gain through the large central skylight with and without shading, illustrating the reduction in heat gain by $\sim 1/3$ achievable through the operation patterns shown above (Figure 7).

penalties caused by late-afternoon warmth. February, which is typically as cold as December but has less direct normal (beam) solar radiation (National Solar Radiation Data Base 2005), showed fewer tendencies to overheat; as a result, its movable insulation schedule followed the prevailing pattern. Together, these results show that movable insulation controlled according to daily hours of sunrise and sunset, without considering heat flux patterns, risks significant heat loss through the windows and skylights it is designed to protect.

Shading, similarly, was optimally activated several hours before the warmest hours of the day to minimize cooling loads; it was subsequently retracted several hours before sunset, remaining retracted throughout the night (Figure 7). Further investigation showed that heat loss through window glass contributed significantly to cooling, and that shading left in place overnight obstructed this cooling. As a result, shading was optimally activated only after the glass had lost as much heat as possible during cool morning hours, and it was optimally retracted as early in the afternoon as the glass could begin to lose heat to the outdoors (Figure 8c and d).

Together, the addition of well-scheduled movable insulation and shading reduced the original heating load by about half and fully compensated for the cooling load introduced by the tilted skylight.

Thermal mass quantity

The third redesign measure investigated the addition of thermal mass in the form of a brick wall under the north side of the skylight (Figure 2) to intercept, store, and later release a portion of the solar radiation collected. The brick wall thickness was optimized simultaneously with movable insulation and shading schedules because previous work had shown strong interdependence among these elements (Rempel and Remington 2015); the optimal value, minimizing the sum of annual heating and cooling loads, was found to be 25cm. This was expected to be an important stabilizing factor, allowing the space to remain within the adaptive thermal comfort zone with less mechanical assistance.

Examination of heat flux into the wall on a typical February week illustrates this effect, showing that the brick wall absorbed and returned several times more energy than the original lightweight gypsum-board wall (Figure 9a). The timing of the winter heat return is striking: while the lightweight wall returned most of its absorbed energy during the afternoon, heat delivery by the heavier brick wall peaked near midnight and continued into the early morning. If evening delivery had been a priority, a less-massive wall would have been preferred, consistent with recent explorations of thermal mass tailored to specific thermal needs (Rempel and Rempel 2013; Rempel et al. 2016). In this case, however, nighttime thermostat setbacks were not employed, causing the optimization to favor a heavier wall to assist with heating during the coldest hours of the day. The mass wall also showed thermal buffering utility during the summer, in which it both absorbed more heat during the day than the lightweight wall, contributing to daytime cooling, and

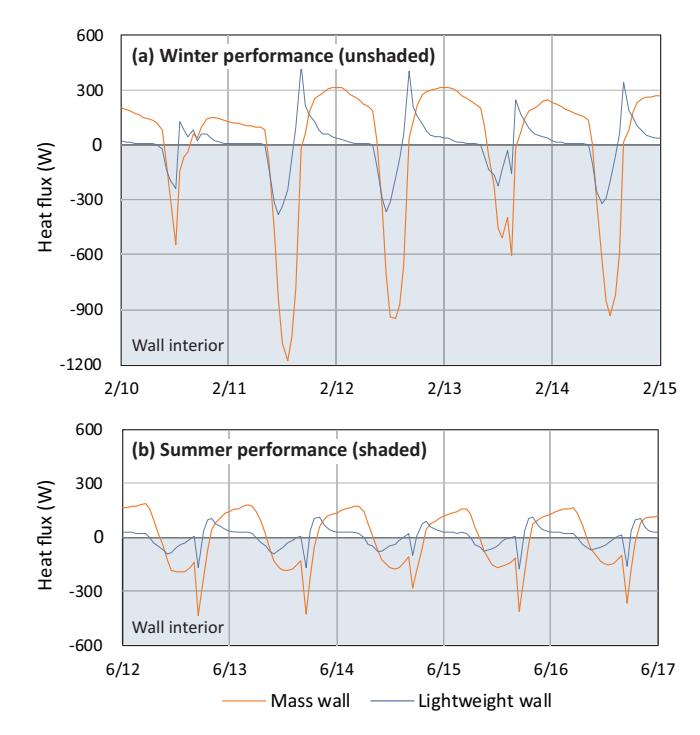


Fig. 9. Heat flux across the surface of the wall underneath the large central skylight in its original lightweight and optimized massive configurations during (a) a typical February week, in which movable insulation was retracted during the day to allow sun to reach the wall, and (b) a typical June week, during which daytime shading diminished solar access to the wall. Negative values show solar energy uptake during the day; positive values show heat delivery into the space in the evening and at night.

released it primarily during the day's coolest early-morning hours (Figure 9b).

Natural ventilation thresholds

The fourth redesign measure addressed natural ventilation for cooling, seeking the thresholds of indoor and outdoor air temperatures beyond which windows should be closed to avoid either overcooling or overheating, respectively. In this case, air temperature thresholds were investigated rather than hourly schedules because previous comparisons have shown them to be more effective (Rempel and Remington 2015). Accordingly, current optimizations showed that natural ventilation should be ceased above outside air temperatures of $\sim 24.5\,^{\circ}\text{C}-26\,^{\circ}\text{C}$ to avoid overheating, as expected (Figure 10a).

Unexpectedly, however, natural ventilation risked overcooling at indoor air temperatures below 23.5 °C–24.5 °C, depending on the month (Figure 10b). This result contrasted to conventional practice, in which natural ventilation during occupied hours is usually discontinued at or near the lower boundary of the thermal comfort zone (e.g., Karlsen et al. 2016). Examination of these results in August, with a typical average monthly outside air temperature of 16.7 °C, illustrated the underlying mechanisms. On a typical late morning, as both outdoor and indoor air temperatures rose, natural

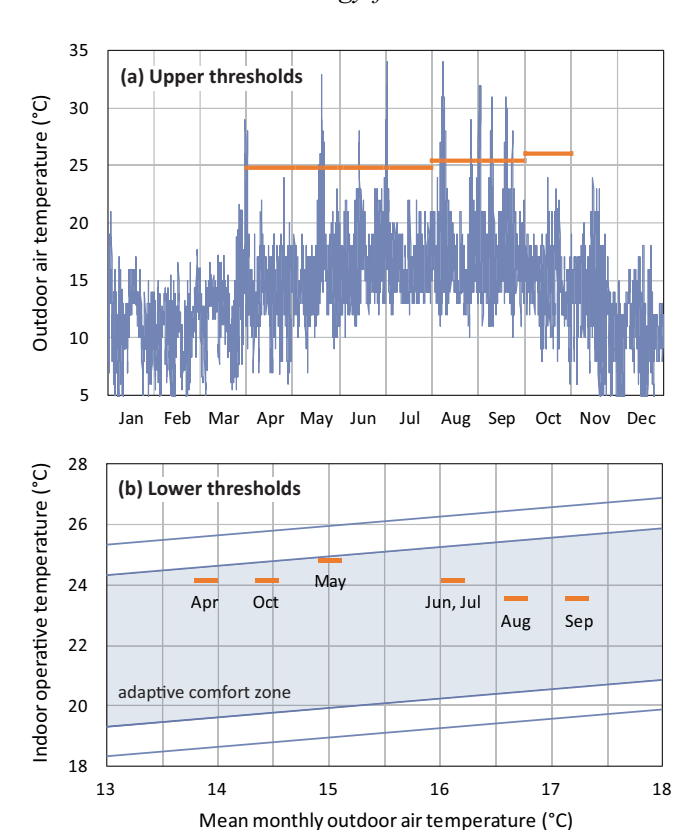


Fig. 10. (a) Typical outdoor temperatures (Oakland CA TMY3) and maximum values above which vents should be closed to avoid overheating, and (b) adaptive thermal comfort zone and minimum indoor temperature values, each month, below which vents should be closed to avoid overcooling.

ventilation effectively removed heat until the outdoor air temperature exceeded the upper bound of the comfort zone, as on 8/27, at which point windows were closed to limit overheating (Figure 11).

As outdoor conditions cooled in the evening, natural ventilation became more effective (and was re-enabled on 8/27), but outdoor temperatures typically dropped so rapidly that natural ventilation had to be discontinued when indoor temperatures reached only the approximate midpoint of the comfort zone to avoid overcooling. Although summer overcooling may be desirable in some circumstances to limit the following day's cooling load (e.g., Wang et al. 2009; Shaviv et al. 2001), optimal thresholds for natural ventilation nevertheless appear likely to depend both on a location's summer diurnal temperature range and on a building's other heat-loss pathways, causing the use of thermal comfort boundaries alone to risk creating discomfort.

Final performance

Together, well-controlled passive heating and cooling systems reduced the expected loads of the building by two-thirds, from 5.6 MWh to 1.8 MWh, with modest investment of embodied energy in the form of a new skylight, movable insulation, shading, and an internal brick wall, and with minimal demand for operational energy. The annual cooling

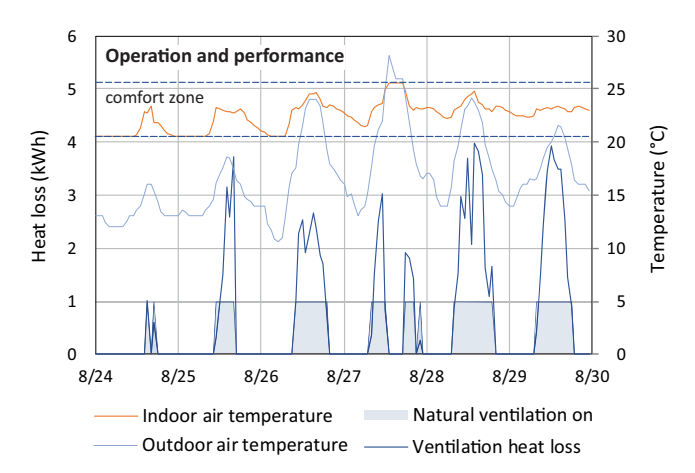


Fig. 11. Natural ventilation operation and performance during a warm August week, showing the opening of windows (shaded areas) in response to outdoor and indoor temperatures under the guidance of operation thresholds shown above (Figure 10).

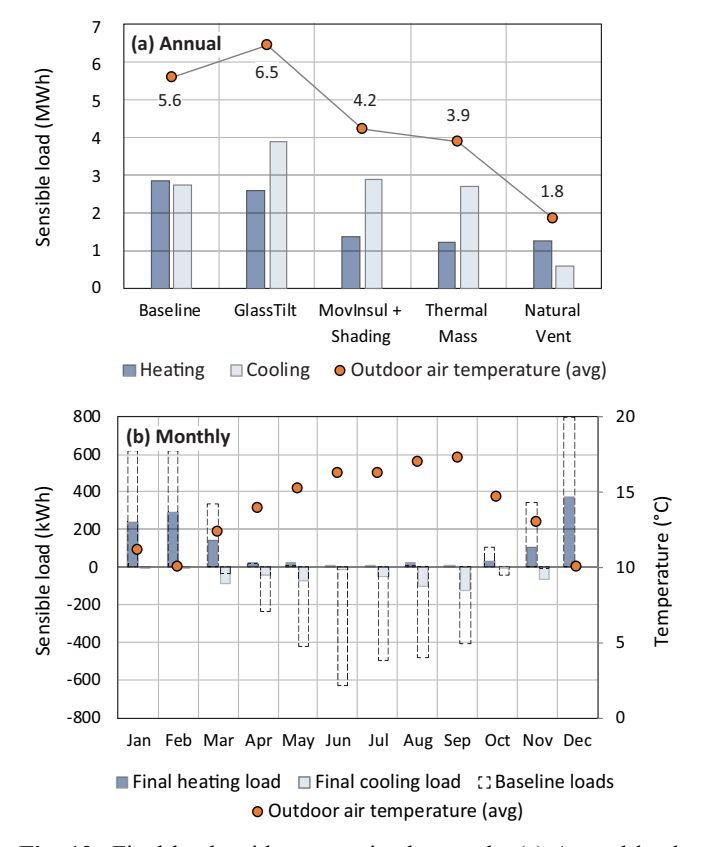


Fig. 12. Final loads with near-optimal controls. (a) Annual loads at each stage, with final reductions of 56% (heating), 79% (cooling), and 67% (total), and (b) final loads by month (see also Figure 5a).

load was reduced by nearly 80%, showing the considerable potential for shading and natural ventilation to offset the anticipated increases in cooling loads in this climate. The annual heating load, in turn, was more than halved, even without expensive, embodied energy-intensive renovations of the existing brick envelope and windows (Figure 12a).

Notably, these controls were not perfect: in optimizing schedules and thresholds for monthly rather than shorter intervals, each day experienced less than ideal control. This is evident, in part, in the appearance of small heating loads in summer resulting from overcooling, and small cooling loads in winter, from overheating (Figure 12b). Instead, these were realistic controls easily manageable either by occupants, assisted by clocks and thermometers, or by actuators signaled similarly only by time or temperature. Still, these controls represented significant improvement over suboptimal strategies, several of which are shown in the Supplementary Information. Shading applied only when inside air temperatures were already warm (>25 °C), for example, was only about 70% as effective as shading applied earlier in the day, while shading applied only when outside temperatures were warm (>25 °C) actually increased the cooling load over the unshaded baseline by interfering with window heat loss in the late afternoon (Figure S1; see Supplementary Information). Natural ventilation supplied only when indoor temperatures rose above the comfort zone, that is, when most people would first notice discomfort, similarly increased the cooling load over the non-ventilated baseline by admitting warm outdoor air. Supplied at lower (though not optimal) temperature thresholds, however, natural ventilation did provide appreciable benefit (Figure S3; see Supplementary Information). These findings show that the operable passive conditioning elements are not necessarily predictive of diminished loads in themselves; rather, well-informed and potentially non-intuitive control strategies, even if not optimal, are necessary for significant benefit to be realized.

Conclusions

The productive use of passive heating and cooling systems can diminish the need for fossil-fueled space conditioning significantly. However, methods with which to find easily manageable control strategies for their operable elements, particularly for buildings without energy management systems, have not yet been established. To address this problem, we have evaluated the use of numerical algorithms for developing simple, near-optimal control strategies for passive systems in the San Francisco Bay area of northern California, revealing several items of importance.

First, the value of optimally-tilted glazing for passive solar heat collection in cloudy climates was reinforced (Figure 6), and the ability of familiar internal roller-blind shading and natural ventilation to compensate for the resulting increase in summer cooling load was confirmed (Figure 12). These findings refute the argument that tilted glazing must be avoided to limit summer cooling loads (e.g., DeKay and Brown 2013; Lechner 2014).

Second, optimal thresholds for operation of movable elements were found not necessarily to be intuitive, and despite current convention, it appears that they cannot be assumed. Here, movable insulation required activation of much greater duration than the "nighttime" (sunset to sunrise) default

assumed in reference books (DeKay and Brown 2013; Balcomb et al. 1984) and in EnergyPlus (U.S. Department of Energy 2016a), as well as other simulation engines (e.g., COMFEN; Grynning et al. 2014). Instead, it was optimally deployed well before sunset, when net heat flux through the glass switched from inward to outward, and remained in place well after sunrise to minimize heat loss during the coldest hours of the day (Figures 7 and 8).

Similarly, shading required activation hours before indoor overheating occurred, in contrast to the comfort threshold-based strategies investigated by Karlsen et al. (2016) and van Moeseke et al. (2007), as well as retraction in the late afternoon to facilitate cooling from window surfaces (Figures 7 and 8). While the use of an incident solar radiation threshold might accomplish such early activation, automated control would then require expensive pyranometers or heat flux sensors for radiation detection, and manual control would require occupants to estimate incident solar radiation levels with some accuracy. Instead, this work shows that schedules based only on time can provide a viable alternative.

Vent open/close thresholds were also found to be non-intuitive, requiring that natural ventilation be discontinued at indoor temperatures well above the lower boundary of the comfort zone (Figure 10b). If the lower boundary had been used as the threshold, as is typical (e.g., Karlsen et al. 2016), over-cooling would have resulted. Outdoor temperature maxima, however, above which ventilation should be discontinued to avoid overheating, were near the upper boundary of the comfort zone as expected (Figure 10a).

Third, the penalties imposed by winter overheating and summer overcooling resulted in optimal monthly schedules that created small summer heating and winter cooling loads (Figure 12b). If modest winter overheating and summer overcooling had been permitted, consistent with the practice of disabling mechanical heating in the summer and viceversa, these off-season loads would have been reduced or eliminated. The load reductions predicted here are therefore conservative. Optimizations conducted over shorter time spans could have addressed this problem, but although these would have appeared productive computationally, they would have complicated daily operation for a relatively minimal amount of benefit.

As a whole, the results above show the striking potential for well-controlled passive strategies to diminish space conditioning loads, even in a building with minimal insulation and appreciable infiltration in a cloudy winter climate. In reducing the heating load by >50% and cooling load by $\sim 80\%$, while maintaining adaptive comfort, the strategies identified challenge the perception that passive systems are difficult to control and, as a result, cannot contribute reliably to comfort. Instead, they suggest the opposite. For California's Mediterranean climates, this shows a path by which building greenhouse gas emissions can be reduced immediately through modest building retrofits, without requiring replacement of natural gas heating systems or adding further demand for renewable electricity resources. Beyond this particular climate, the value of well-operated

elements for passive space-conditioning is expected to be widespread in climates with significant diurnal and seasonal temperature variation, and the method for finding straightforward, effective control strategies is valid in general.

Funding

This work was supported in part by the National Science Foundation through grant number CBET-1804218: Climate-Responsive Design and Control Strategies for Affordable Multi-Family Residences.

ORCID

Alexandra R. Rempel (b) http://orcid.org/0000-0002-2733-2449

References

Ackerly, D., A. Jones, M. Stacey, and B. Riordan. 2018. San Francisco Bay Area Summary Report, *California's Fourth Climate Change Assessment*. Berkeley, CA: University of California, Berkeley. Publication CCCA4-SUM-2018-005.

ANSI/ASHRAE. 2017. Standard 55-2017. Thermal environmental conditions for human occupancy. ISSN 1041-2336. Atlanta, GA: ASHRAE.

ASHRAE. 2013. ASHRAE Handbook of Fundamentals. Atlanta, GA: ASHRAE.

Balcomb, J.D., R.W. Jones, R.D. McFarland, and W.O. Wray. 1984.
Passive Solar Heating Analysis: A Design Manual. Los Alamos NM and Atlanta GA: Los Alamos National Laboratory and the ASHRAE.

Big Ladder Software. 2017. Euclid v0.9.3. https://bigladdersoftware.com/projects/euclid/.

Bushnell, D. 1990. GENOPT—a program that writes user-friendly optimization code. *International Journal of Solids and Structures* 26:1173–210.

California Energy Commission. 2018. Energy efficiency programs, State of California. http://www.energy.ca.gov/efficiency/.

Carmody, J., S. Selkowitz, D. Arasteh, and L. Heschong. 2007. Residential Windows: A Guide to New Technologies and Energy Performance. New York: WW Norton & Company.

Chahwane, L., Stephan, L., Wurtz, E., Zuber, B. 2011. On a novel approach to control natural and mechanical night ventilation. *12th IBPSA Conference*, Sydney, Australia, November 14–16.

DeKay, M., and G.Z. Brown. 2013. Sun, Wind, and Light: Architectural Design Strategies. New York: John Wiley & Sons.

Djuric, N., V. Novakovic, J. Holst, and Z. Mitrovic. 2007. Optimization of energy consumption in buildings with hydronic heating systems considering thermal comfort by use of computerbased tools. *Energy and Buildings* 39:471–7.

Duffie, J.A., and W.A. Beckman. 2013. *Solar Engineering of Thermal Processes*. New York: John Wiley & Sons.

Executive Order B-55-18. 2018. To Achieve Carbon Neutrality. Governor Jerry Brown, State of California, September 10.

Eymet, V., J.L. Dufresne, P. Ricchiazzi, R. Fournier, and S. Blanco. 2004. Long-wave radiative analysis of cloudy scattering atmospheres using a net exchange formulation. *Atmospheric Research* 72(1-4): 239–61.

Goswami, D.Y., F. Kreith, and J.F. Kreider. 2000. *Principles of Solar Engineering*. 2nd Ed., Passive methods for heating, cooling, and daylighting. Philadelphia PA: Taylor & Francis, pp. 297–336.

- Grynning, S., B. Time, and B. Matusiak. 2014. Solar shading control strategies in cold climates—Heating, cooling demand and daylight availability in office spaces. *Solar Energy* 107:182–94.
- Hoegh-Guldberg, O., D. Jacob, M. Taylor, M. Bindi, S. Brown, I. Camilloni, A. Diedhiou, R. Dialante, K. Ebi, F. Engelbrecht, J. Guiot, Y. Hijioka, S. Mehrotra, A. Payne, S.I. Seneviratne, A. Thomas, R. Warren, and G. Zhou. 2018. Global Warming of 1.5°C: An IPCC Special Report on the Impacts of Global Warming of 1.5°C Above Pre-Industrial Levels and Related Global Greenhouse Gas Emission Pathways, in the Context of Strengthening the Global Response to the Threat of Climate Change, Sustainable Development, and Efforts to Eradicate Poverty, Impacts of 1.5°C global warming on natural and human systems. V. Masson-Delmotte, P. Zhai, H. O. Pörtner, D. Roberts, J. Skea, P.R. Shukla, A. Pirani, W. Moufouma-Okia, C. Péan, R. Pidcock, S. Connors, J. B. R. Matthews, Y. Chen, X. Zhou, M. I. Gomis, E. Lonnoy, T. Maycock, M. Tignor, and T. Waterfield, eds. Washington, DC: U.S. Global Change Research Program. doi:10.7930/NCA4.2018.
- Hopkins, A.S., K. Takahashi, D. Glick, and M. Whited. 2018. Decarbonization of Heating Energy Use in California Buildings. Syngenta Energy Economics, Inc. New York: Natural Resources Defense Council.
- International Commission on Illumination. 2003. Spatial distribution of daylight - CIE Standard General Sky. ISO 15469:2004(E)/CIE S 011/E:2003. Geneva, Switzerland: International Organization for Standardization.
- Kämpf, J.H., M. Wetter, and D. Robinson. 2010. A comparison of global optimization algorithms with standard benchmark functions and real-world applications using EnergyPlus. *Journal of Building Performance Simulation* 3(2):103–20.
- Karlsen, L., P. Heiselberg, I. Bryn, and H. Johra. 2016. Solar shading control strategy for office buildings in cold climate. *Energy and Buildings* 118:316–28.
- Lawrence Berkeley National Laboratory. 2017. Window: A computer program for calculating total window thermal performance indices. https://windows.lbl.gov/software/window.
- Lechner, N. 2014. Heating, Cooling, Lighting: Sustainable Design Methods for Architects, 4th Ed., Ch. 7: Passive solar. Hoboken, NJ: Wiley.
- Littlefair, P., J. Ortiz, and C.D. Bhaumik. 2010. A simulation of solar shading control on UK office energy use. *Building Research & Information* 38:638–46.
- National Solar Radiation Data Base, 2005. 1991- 2005 Update: Typical Meteorological Year 3; Oakland Metropolitan Airport. https://rredc.nrel.gov/solar/old_data/nsrdb/1991-2005/tmy3/.
- Ochoa, C.E., and I.G. Capeluto. 2008. Strategic decision-making for intelligent buildings: Comparative impact of passive design strategies and active features in a hot climate. *Building and Environment* 43:1829–39.
- Peel, M.C., B.L. Finlayson, and T.A. McMahon. 2007. Updated world map of the Köppen-Geiger climate classification. *Hydrology and Earth System Sciences Discussions* 4(2):439–73.
- Perez, R., P. Ineichen, R. Seals, J. Michalsky, and R. Stewart. 1990. Modeling daylight availability and irradiance components from direct and global irradiance. *Solar Energy* 44:271–89.
- Rahadian, K., and M.I. Alhamid. 2015. Simulation and optimization of a solar thermal cooling system in a manufacturing research center building to reduce operational cost using software EnergyPlus and GenOpt. *Applied Mechanics and Materials* 780:81–6.
- Regional Plan Association. 2018. Megaregions: Northern California. http://www.america2050.org/northern_california.html.
- Rempel, A.R., and S. Lim. 2018. Optimal control strategies for passive heating and cooling elements reduce loads by two-thirds in the adaptive reuse of a San Francisco Bay area office. *Proceedings of the 7th International Building Physics Conference, Syracuse NY, September 23–26.*

- Rempel, A.R., and S.J. Remington. 2015. Optimization of passive cooling control thresholds with GenOpt and EnergyPlus. *Proceedings of the Symposium on Simulation in Architecture and Urban Design*, Washington, DC, April 12–15, pp.103–10.
- Rempel, A.R., and A.W. Rempel. 2013. Rocks, clays, water, and salts: Highly durable, infinitely rechargeable, eminently controllable thermal batteries for buildings. *Geosciences* 3(1):63–101.
- Rempel, A.R., A.W. Rempel, K.V. Cashman, K.N. Gates, C.J. Page, and B. Shaw. 2013. Interpretation of passive solar field data with EnergyPlus models: Un-conventional wisdom from four sunspaces in Eugene, Oregon. *Building and Environment* 60:158–72.
- Rempel, A.R., A.W. Rempel, K.R. Gates, and B. Shaw. 2016. Climate-responsive thermal mass design for Pacific Northwest sunspaces. *Renewable Energy* 85:981–93.
- Santamouris, M., A. Sfakianaki, and K. Pavlou. 2010. On the efficiency of night ventilation techniques applied to residential buildings. *Energy and Buildings* 42:1309–13.
- Schulze, T., and U. Eicker. 2013. Controlled natural ventilation for energy efficient buildings. Energy and Buildings 56:221–32.
- Schulze, T., D. Gürlich, and U. Eicker.2018. Performance assessment of controlled natural ventilation for air quality control and passive cooling in existing and new office type buildings. *Energy and Buildings* 172:265–78.
- Shaviv, E., A. Yezioro, and I.G. Capeluto. 2001. Thermal mass and night ventilation as passive cooling design strategy. *Renewable Energy* 24:445–52.
- Stevanović, S. 2013. Optimization of passive solar design strategies. *Renewable and Sustainable Energy Reviews* 25:177–96.
- Tzempelikos, A., and A.K. Athienitis. 2007. The impact of shading design and control on building cooling and lighting demand. Solar Energy 81:369–82.
- U.S. Department of Energy. 2016a. EnergyPlus Input Output Reference, v8.7. https://bigladdersoftware.com/epx/docs/8-7/inputoutput-reference/index.html.
- U.S. Department of Energy. 2016b. EnergyPlus. https://energyplus.net/.
- U.S. Energy Information Administration. 2018a. Consumption by Sector. http://www.eia.gov/totalenergy/data/monthly/
- U.S. Energy Information Administration. 2018b. California State Profile and Energy Estimates; Rankings: Total Carbon Dioxide Emissions, 2015. http://www.eia.gov/state/rankings/?sid=CA#series/226
- U.S. Energy Information Administration. 2015. Residential Energy Consumption Survey: Table CE3.1 End-use consumption in the U.S. https://www.eia.gov/consumption/residential/data/2015/index. php?view=consumption.
- U.S. Global Change Research Program. 2018. 2018: Impacts, Risks, and Adaptation in the United States: Fourth National Climate Assessment, Volume II, D.R. Reidmiller, C.W. Avery, D.R. Easterling, K.E. Kunkel, K.L.M. Lewis, T.K. Maycock, and B.C. Stewart, eds. Washington, DC: U.S. Global Change Research Program, 1515 pp. doi: 10.7930/NCA4.2018
- van Moeseke, G., I. Bruyère, and A. DeHerde. 2007. Impact of control rules on the efficiency of shading devices and free cooling for office buildings. *Building and Environment* 42:784–93.
- Wang, Z., L. Yi, and F. Gao. 2009. Night ventilation control strategies in office buildings. Solar Energy 83(10):1902–13.
- Western Regional Climate Center. 2016. Berkeley, California. https://wrcc.dri.edu/cgi-bin/cliMAIN.pl?ca0693.
- Wetter, M. 2016. GenOpt Generic Optimization Program User Manual, v3.1.1. Simulation Research Group, Building Technologies Division. Berkeley, CA: Lawrence Berkeley National Laboratory. http://simulationresearch.lbl.gov/GO/index.html.
- Wetter, M., and J. Wright. 2003. Comparison of a generalized pattern search and a genetic algorithm optimization method. *Proceedings of the 8th International IBPSA Conference, Eindhoven, Netherlands, August 2003*, pp. 1401–08.
- World Population Review. 2018. San Francisco Population 12-07-2018. http://worldpopulationreview.com/us-cities/san-francisco/.